

Analyzing Faulted Transmission Lines: Phase Components as an Alternative to Symmetrical Components

Steven Chase, Sumit Sawai, and Amol Kathe
Schweitzer Engineering Laboratories, Inc.

© 2018 IEEE. Personal use of this material is permitted. Permission from IEEE must be obtained for all other uses, in any current or future media, including reprinting/republishing this material for advertising or promotional purposes, creating new collective works, for resale or redistribution to servers or lists, or reuse of any copyrighted component of this work in other works.

This paper was presented at the 71st Annual Conference for Protective Relay Engineers and can be accessed at: <https://doi.org/10.1109/CPRE.2018.8349771>.

For the complete history of this paper, refer to the next page.

Presented at the
72nd Annual Georgia Tech Protective Relaying Conference
Atlanta, Georgia
May 2–4, 2018

Previously presented at the
71st Annual Conference for Protective Relay Engineers, March 2018

Previous revised edition released October 2017

Originally presented at the
44th Annual Western Protective Relay Conference, October 2017

Analyzing Faulted Transmission Lines: Phase Components as an Alternative to Symmetrical Components

Steven Chase, Sumit Sawai, and Amol Kathe, *Schweitzer Engineering Laboratories, Inc.*

Abstract—Protection engineers are often interested in calculating the steady-state voltages and currents on faulted transmission lines. This necessitates the use of accurate fault solution techniques. The most commonly taught and used methods involve symmetrical components. Symmetrical components are advantageous in that they yield multiple decoupled systems that are simple to solve. This simplicity was crucial before the advent of digital computers. With modern computers, it is equally easy to perform calculations with phase components (A, B, C) or with symmetrical components (positive, negative, zero). With symmetrical components, different circuit topologies must be used for different fault types, which can be inconvenient in practice. Additionally, symmetrical component techniques commonly assume line transposition and give oversimplified results for real-life cases.

This paper presents phase-domain solution methods as an alternative to symmetrical components. Phase-domain analysis allows all ten common shunt faults to be modeled using a single circuit topology. In exchange for this convenience, the phase-domain approach must account for mutual coupling between the three phases of a transmission line. However, this in turn allows phase-domain analysis to be used to model untransposed transmission lines without compromising the accuracy of the solution.

This paper presents a general derivation for a steady-state, phase-domain transmission line solution and illustrates its practical use through several examples. Steady-state signals can be reliably used for testing traditional phasor-based relays. This steady-state solution is then translated into a time-domain equivalent, which numerically solves differential equations to accurately model the transition between prefault and fault states. Accurate modeling of state transitions makes this solution suitable for testing relays that use incremental quantities.

I. INTRODUCTION

Modern, microprocessor-based line protective relays implement a variety of sophisticated protection functions. A few examples of such functions include the following:

- Distance elements
- Directional elements
- Fault location

In order to test such protection functions, it is necessary to supply secondary voltage and current signals that have the correct magnitudes and relative phase relationships to the relay. In addition, it is often necessary to simulate both prefault and fault conditions and to accurately model the changes in the voltages and currents from one state to the next.

This testing requires simulating a power system and using the simulation results to generate test signals. There are numerous solutions that meet this need, ranging from non-real-time transient analysis software programs run on PC computers to real-time simulators run on dedicated hardware. These applications are very general and powerful, allowing users to build and simulate arbitrarily complex power systems using graphical user interfaces (GUI). Additionally, component models within these simulation products can be quite complex and can require users to enter simulation parameters that are not of immediate interest.

In many cases, such as bench testing with a secondary test set, relatively few simulation parameters are of immediate interest. The following are some essential line and fault parameters:

- Line positive- and zero-sequence impedances
- Per-unit fault locations
- Source voltage magnitudes and phase angles
- Fault type and fault resistance

In such simple cases, it is neither necessary nor desirable to explicitly account for complexities such as transmission line geometry and soil resistivity. These are implicitly encapsulated within the given essential line parameters, and it is often convenient for an engineer or test technician to simply declare these values.

Additionally, certain system topologies, such as the classic two-source system with a transmission line, are used very frequently in simulations. Because engineers and technicians are often interested in only a few simulation parameters and because certain classic topologies are frequently used, handcrafted signal solvers can be very useful for supplementing more sophisticated and more demanding simulation tools. These solvers allow common fault scenarios to be simulated quickly and with minimal effort.

Historically, engineering practice and education have relied heavily on symmetrical components for faulted transmission line analysis. The principal reason for this is the ability of symmetrical components to resolve an electromagnetically coupled, three-phase power system into a superposition of three decoupled power systems. These decoupled sequence networks (positive, negative, zero) are ideally suited to handwritten analysis.

In the modern computer age, the coupling between the three phases (A, B, and C) is less problematic, given the ability of software programs to solve relatively large linear systems with complex numbers as matrix entries. In addition, phase domain analysis offers several advantages over symmetrical components. A key advantage among these is the ability to model all ten common shunt faults using a single circuit topology.

Section II of this paper introduces a simple, two-source power system model with a single transmission line that serves as an example system to demonstrate the differences between sequence-domain analysis and phase-domain analysis. This section also establishes some general nomenclature that is used throughout this paper.

Section III briefly reviews symmetrical component analysis for faults on the system presented in Section II. This section illustrates the benefits and disadvantages of symmetrical component analysis.

Section IV introduces a general shunt fault model that is used in faulted transmission line phase-domain analysis. This section presents a derivation for a system of linear equations that, when solved, yields the fault current for any of the ten standard shunt faults. These equations are applicable to the generation of steady-state fault signals that are useful for testing traditional phasor-based relays. We present derivations for transposed and untransposed lines.

Section V presents test results for the single-circuit phase-domain solver. All ten shunt fault types were simulated and tested with a distance relay.

Section VI develops a double-circuit, phase-domain model consisting of two parallel transmission lines with common buses on both ends.

Section VII presents test results for the double-circuit, phase-domain solver. Examples illustrate the effect of zero-sequence mutual coupling on relay impedance calculations.

Section VIII translates the two-source, single-line, steady-state model into an equivalent time-domain model. The time-domain model uses a state-space representation of the power system and implements numerical integration to solve for the time-varying currents and voltages on a faulted transmission line.

Sections IX and X discuss the application of the phase-domain solver to the testing of time-domain, incremental quantity-based protection functions. Both ac steady-state and time-domain variants of the solver were tested, and the results presented in these sections illustrate the impact of the prefault to fault state transition on the time-domain incremental quantities and associated directional elements.

Finally, we provide some key conclusions.

II. BASIC POWER SYSTEM MODEL AND NOMENCLATURE

Fig. 1 illustrates the basic power system model that is central to the analysis presented in this paper. The model consists of two solidly grounded, three-phase system sources at the ends of

a single transmission line. The source on the left is designated “S,” and the source on the right is designated “R.” There are two virtual relays at the line ends that are also designated “S” and “R.”

For the system sources and the line, the phase-to-phase electromagnetic couplings are assumed to be identical, resulting in only two impedance parameters for each element: a self-impedance and a mutual impedance. The self-impedance and mutual impedance for System Source S are Z_{SS} and Z_{MS} , respectively. The self-impedances and mutual impedances for System Source R are Z_{SR} and Z_{MR} , respectively. The self-impedances and mutual impedances for the transmission line are Z_S and Z_M , respectively.

These parameters correspond to an ideally transposed line (this assumption is relaxed in Section IV). For practical purposes, this system can be regarded as three ideally transposed transmission line segments in series with two ideal voltage sources. Of course, this arrangement does not exactly correspond to a real power system, but it is adequate for the general testing of line protective relays.

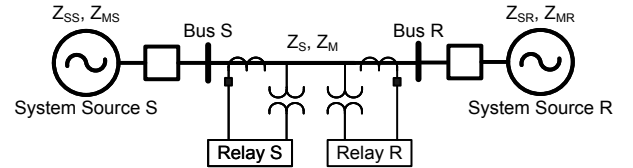


Fig. 1. Two-source power system with one transmission line

III. FAULT ANALYSIS USING SYMMETRICAL COMPONENTS

This section provides a very brief overview of some of the key aspects of fault analysis using symmetrical components. There is a vast amount of existing literature on this topic. Indeed, the fields of protective relaying and power system analysis have largely been built on these symmetrical component principles over roughly the past hundred years. Some introductory texts and papers on this subject include [1], [2], and [3].

The phenomenon of mutual electromagnetic coupling is fundamentally important in motivating the use of symmetrical components for power system analysis. Consider the change in voltage (voltage drop) over the length of a transmission line resulting from the current flowing through it. The voltage drop in a particular phase (e.g., Phase A) depends not only on the current flowing in Phase A but also on the current flowing in the neighboring Phases B and C. This phenomenon makes three-phase systems difficult to analyze in the phase-domain without the aid of computer software.

Fig. 2 illustrates the voltages and currents during a Phase-C-to-ground fault on a three-phase transmission line. Notice that the voltages in Phases A and B are disturbed, even though there are no prominent disturbances in the Phase A and Phase B currents. The change in the Phase C current alters the Phase A and Phase B voltages via electromagnetic coupling.

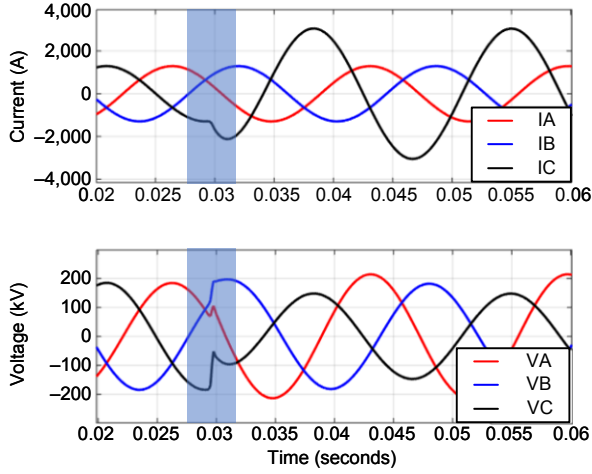


Fig. 2. Electromagnetic coupling illustration

The relationship between the Phase A voltage drop and the Phase A current is encapsulated in the self-impedance of the transmission line. The relationship between the Phase A voltage drop and the Phase B and Phase C currents is encapsulated by the mutual impedance of the transmission line. Similar statements can be made for the Phase B and Phase C voltage drops. Equation (1) illustrates this mathematically. The voltage and current quantities in (1) are complex vectors, but for convenience, they are represented without vector notation, relying instead on capital letters to denote complex values. The terms V_{SRA} , V_{SRB} , and V_{SRC} are the voltage drops over the length of the transmission line (see Fig. 1).

$$\begin{bmatrix} V_{SRA} \\ V_{SRB} \\ V_{SRC} \end{bmatrix} = \begin{bmatrix} Z_S & Z_M & Z_M \\ Z_M & Z_S & Z_M \\ Z_M & Z_M & Z_S \end{bmatrix} \cdot \begin{bmatrix} I_A \\ I_B \\ I_C \end{bmatrix} \quad (1)$$

Recall the transformation between phase-domain (A, B, C) and sequence-domain (zero [0], positive [1], and negative [2]) quantities for an ABC phase rotation as shown in (2). This transformation is equally applicable to both voltages and currents. The equations are written considering Phase A as the reference, and we follow this same convention throughout the paper.

$$\begin{bmatrix} qA \\ qB \\ qC \end{bmatrix} = \begin{bmatrix} 1 & 1 & 1 \\ 1 & a^2 & a \\ 1 & a & a^2 \end{bmatrix} \cdot \begin{bmatrix} q0 \\ q1 \\ q2 \end{bmatrix} = [A] \cdot \begin{bmatrix} q0 \\ q1 \\ q2 \end{bmatrix} \quad (2)$$

$$\begin{bmatrix} q0 \\ q1 \\ q2 \end{bmatrix} = \frac{1}{3} \cdot \begin{bmatrix} 1 & 1 & 1 \\ 1 & a & a^2 \\ 1 & a^2 & a \end{bmatrix} \cdot \begin{bmatrix} qA \\ qB \\ qC \end{bmatrix} = [A^{-1}] \cdot \begin{bmatrix} qA \\ qB \\ qC \end{bmatrix}$$

where:

$$a = e^{j \cdot 120^\circ}$$

$$j = \sqrt{-1}$$

q = voltage or current

Replacing the phase quantities in (1) with the sequence quantities via matrix transformation yields the relationship between the sequence voltage drops and the sequence currents,

shown in (3). For an ideally transposed line, the transmission line voltage drop in each sequence depends only on the current in that same sequence (i.e., the zero-sequence voltage drop depends only on the zero-sequence current). This is the principal advantage of symmetrical component analysis. Symmetrical components split a coupled system, which is difficult to solve by hand, into three decoupled systems, each of which is relatively easy to solve without the aid of advanced tools.

$$[A] \begin{bmatrix} V_{SR0} \\ V_{SR1} \\ V_{SR2} \end{bmatrix} = \begin{bmatrix} Z_S & Z_M & Z_M \\ Z_M & Z_S & Z_M \\ Z_M & Z_M & Z_S \end{bmatrix} \cdot [A] \cdot \begin{bmatrix} I_0 \\ I_1 \\ I_2 \end{bmatrix}$$

$$\begin{bmatrix} V_{SR0} \\ V_{SR1} \\ V_{SR2} \end{bmatrix} = [A^{-1}] \begin{bmatrix} Z_S & Z_M & Z_M \\ Z_M & Z_S & Z_M \\ Z_M & Z_M & Z_S \end{bmatrix} \cdot [A] \cdot \begin{bmatrix} I_0 \\ I_1 \\ I_2 \end{bmatrix} \quad (3)$$

$$\begin{bmatrix} V_{SR0} \\ V_{SR1} \\ V_{SR2} \end{bmatrix} = \begin{bmatrix} Z_0 & 0 & 0 \\ 0 & Z_1 & 0 \\ 0 & 0 & Z_2 \end{bmatrix} \cdot \begin{bmatrix} I_0 \\ I_1 \\ I_2 \end{bmatrix}$$

where:

$$Z_0 = Z_S + 2 \cdot Z_M$$

$$Z_1 = Z_2 = Z_S - Z_M$$

We now show, without derivation, some of the classic sequence network representations of common shunt faults. Fig. 3, Fig. 4, and Fig. 5 illustrate the sequence networks for an AG fault (Phase-A-to-ground), a BC fault (Phase-B-to-Phase-C), and a BCG fault (Phase-B-to-Phase-C-to-ground), respectively [4]. These figures each show a two-source network with a single transmission line. The transmission line is faulted at a per-unit location denoted as m . For example, a fault at 50 percent of the line length relative to Relay S has an associated m value of 0.5 pu. Because the system sources produce only positive-sequence voltage, only the positive-sequence network contains sources. In these figures, R_F refers to the fault resistance.

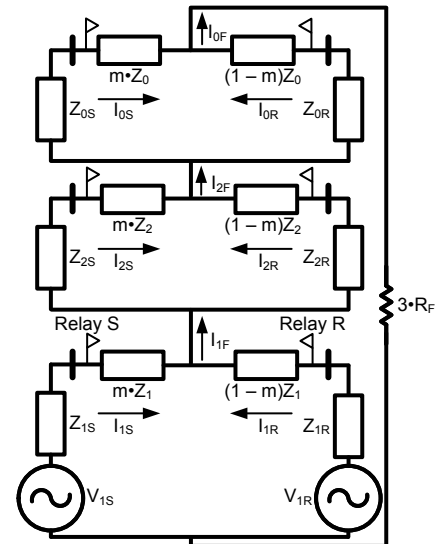


Fig. 3. Sequence networks for an AG fault

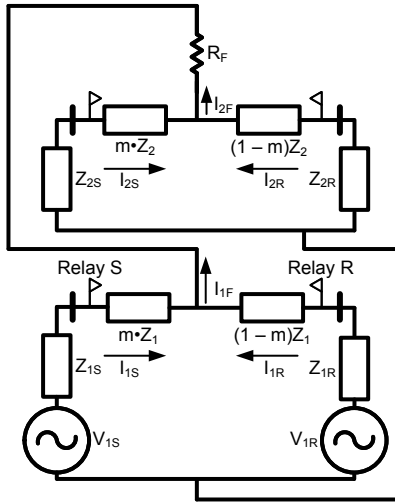


Fig. 4. Sequence networks for a BC fault

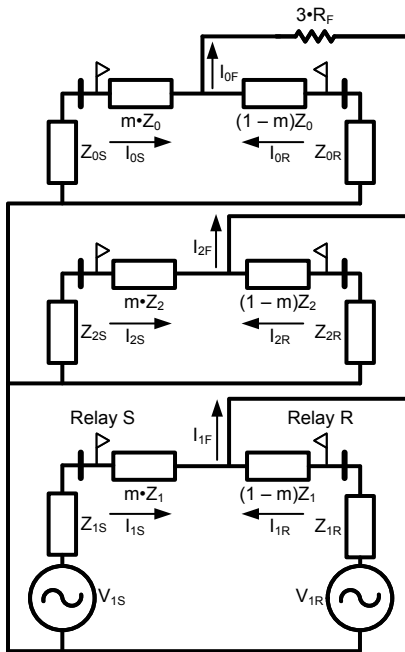


Fig. 5. Sequence networks for a BCG fault

These figures clearly illustrate that different fault types result in different topologies when the power system is represented in terms of sequence networks. For the shunt faults, the zero-sequence network is only present when the ground is involved. The positive-sequence and negative-sequence networks are in series for single-line-to-ground faults and are parallel (neglecting fault resistance) for line-to-line faults.

Additionally, the relationships between the sequence quantities depend on which family the fault falls into. AG, BC, and BCG faults are most naturally described in terms of sequence quantities using Phase A as the reference (e.g., $I_0, I_1, I_2 = I_{A0}, I_{A1}, I_{A2}$). Fig. 3, Fig. 4, and Fig. 5 thus illustrate the relationships between the Phase A sequence quantities. For a BG fault, the symmetrical component diagram would show the Phase B sequence quantities (e.g., $I_0, I_1, I_2 = I_{B0}, I_{B1}, I_{B2}$). To get back to the Phase A sequence quantities from the Phase B quantities requires a phase rotation.

A general process outline for solving shunt faults using symmetrical components is as follows (note that there is some flexibility, subject to individual preference):

1. Connect the sequence networks together appropriately, given the fault type.
2. Determine the Thevenin equivalent circuit for each sequence network.
3. Condense the impedances from the three Thevenin circuits into a total network impedance.
4. Use Ohm's law to calculate the total fault current from the positive-sequence voltage and the total network impedance.
5. Use current division to determine how the total fault current splits between the S and R terminals.
6. If the fault is not within the Phase A family, apply phase rotations as necessary to get back to the classic, symmetrical components (e.g., $I_0, I_1, I_2 = I_{A0}, I_{A1}, I_{A2}$) and ultimately back to the phase domain (A, B, C).

While the decoupling of the sequence networks is very useful for engineers who want to perform calculations by hand, there can be considerable complexity involved with the fault calculations (outlined in Bullets 1 through 6 listed previously). This complexity derives primarily from the fact that the circuit topology varies with the fault type.

IV. FAULT ANALYSIS IN THE PHASE DOMAIN

Fig. 6 shows a three-phase power system that forms the basis of the analysis presented in this section. The voltage system sources $V_{AS}, V_{BS},$ and V_{CS} drive the circuit on the S side, and the voltage sources $V_{AR}, V_{BR},$ and V_{CR} drive the circuit on the R side. The S-side currents are $I_{AS}, I_{BS},$ and I_{CS} , and the R-side currents are $I_{AR}, I_{BR},$ and I_{CR} . The S-side system source has self-impedance Z_{SS} and mutual impedance Z_{MS} , and the R-side system source has self-impedance Z_{SR} and mutual impedance Z_{MR} . The self-impedances and mutual impedances of the transmission line are Z_S and Z_M , respectively. The per-unit distance to the fault is m . Virtual relays are located at the S and R terminal power system buses.

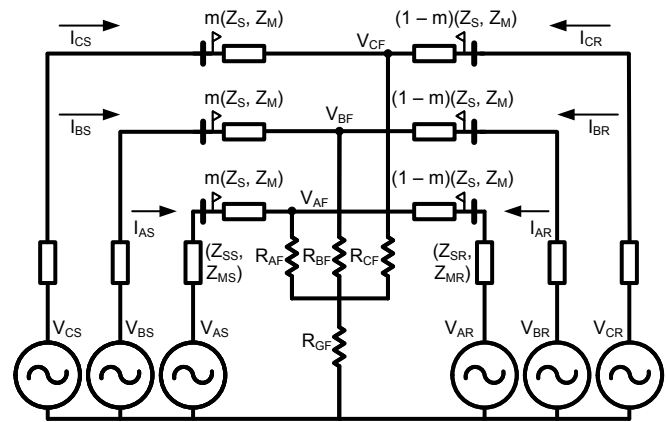


Fig. 6. Three-phase power system representation with fault circuit

The fault circuit in Fig. 6 can be used to simulate any of the ten common shunt faults (AG, BG, CG, AB, BC, CA, ABG,

BCG, CAG, and ABC). Reference [5] presents the same fault circuit, also in the context of phase-domain analysis.

In this scenario, the mutual impedances between the phases are equal, and the relationships between (Z_1, Z_0) and (Z_S, Z_M) are as expressed in (4). Similar relationships hold for the system source impedances, because the system source impedances are modeled as transmission line segments for convenience. Note that for this analysis, we have effectively transitioned from the sequence domain to the phase domain, and we have embraced the mutual coupling instead of avoiding it by using transformations.

$$\begin{aligned} Z_S &= \frac{1}{3}(Z_0 + 2Z_1) \\ Z_M &= \frac{1}{3}(Z_0 - Z_1) \end{aligned} \quad (4)$$

Fig. 7 illustrates the values R_{AF} , R_{BF} , R_{CF} , and R_{GF} that correspond to the bolted AG, BC, and CAG faults, as well as to the prefault condition. Other line-to-ground, line-to-line, and line-to-line-to-ground faults can be modeled similarly. In practice, large, finite numbers can be used in place of infinity.

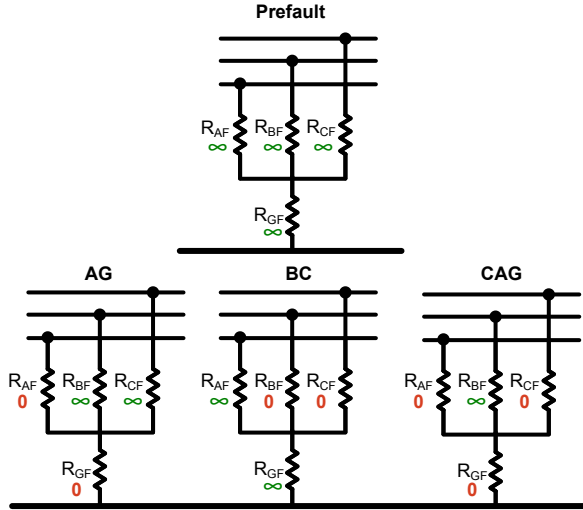


Fig. 7. Modeling various shunt faults using the three-phase fault circuit

When solving the circuit in Fig. 6, the objective is to determine the three-phase voltages and currents at Relays S and R. We therefore solve for six steady-state currents and six steady-state voltages, all of which are represented as complex numbers in the ac steady-state solution. This solution consists of the following steps:

1. Write six linear Kirchoff's voltage law (KVL) equations that describe the power system.
2. Represent the system in matrix form ($Ax = B$).
3. Solve the linear system for the six unknown currents.
4. Using the system currents, calculate the voltages at the power system buses (the virtual relay locations) by accounting for the voltage drops over the source impedances.

We begin by writing and equating expressions for the phase voltages at the fault point (V_{AF} , V_{BF} , and V_{CF}), as seen from the S side and the R side. The equations in (5) show the expressions for the fault voltages.

$$\begin{aligned} V_{AF_S} &= V_{AS} - Z_{SS} \cdot I_{AS} - Z_{MS}(I_{BS} + I_{CS}) \\ &\quad - m \cdot Z_S \cdot I_{AS} - m \cdot Z_M(I_{BS} + I_{CS}) \\ V_{BF_S} &= V_{BS} - Z_{SS} \cdot I_{BS} - Z_{MS}(I_{AS} + I_{CS}) \\ &\quad - m \cdot Z_S \cdot I_{BS} - m \cdot Z_M(I_{AS} + I_{CS}) \\ V_{CF_S} &= V_{CS} - Z_{SS} \cdot I_{CS} - Z_{MS}(I_{AS} + I_{BS}) \\ &\quad - m \cdot Z_S \cdot I_{CS} - m \cdot Z_M(I_{AS} + I_{BS}) \\ V_{AF_R} &= V_{AR} - Z_{SR} \cdot I_{AR} - Z_{MR}(I_{BR} + I_{CR}) \\ &\quad - (1-m)Z_S \cdot I_{AR} - (1-m)Z_M(I_{BR} + I_{CR}) \\ V_{BF_R} &= V_{BR} - Z_{SR} \cdot I_{BR} - Z_{MR}(I_{AR} + I_{CR}) \\ &\quad - (1-m)Z_S \cdot I_{BR} - (1-m)Z_M(I_{AR} + I_{CR}) \\ V_{CF_R} &= V_{CR} - Z_{SR} \cdot I_{CR} - Z_{MR}(I_{AR} + I_{BR}) \\ &\quad - (1-m)Z_S \cdot I_{CR} - (1-m)Z_M(I_{AR} + I_{BR}) \end{aligned} \quad (5)$$

Equating these expressions gives (6):

$$\begin{aligned} V_{AF_S} &= V_{AF_R} \rightarrow V_{AF_S} - V_{AF_R} = 0 \\ V_{BF_S} &= V_{BF_R} \rightarrow V_{BF_S} - V_{BF_R} = 0 \\ V_{CF_S} &= V_{CF_R} \rightarrow V_{CF_S} - V_{CF_R} = 0 \end{aligned} \quad (6)$$

The equations in (6) show the first three equations in the linear system. To form the next three equations, we create KVL loops that begin at the reference bus and travel through the S-side system sources, the line on the S-side of the fault, and the fault impedance before returning to the reference bus. The equations in (7) show the result.

$$\begin{aligned} V_{AS} - Z_{SS} \cdot I_{AS} - Z_{MS}(I_{BS} + I_{CS}) \\ - m \cdot Z_S \cdot I_{AS} - m \cdot Z_M(I_{BS} + I_{CS}) - R_{AF}(I_{AS} + I_{AR}) \\ - R_{GF}(I_{AS} + I_{AR} + I_{BS} + I_{BR} + I_{CS} + I_{CR}) = 0 \end{aligned}$$

$$\begin{aligned} V_{BS} - Z_{SS} \cdot I_{BS} - Z_{MS}(I_{AS} + I_{CS}) \\ - m \cdot Z_S \cdot I_{BS} - m \cdot Z_M(I_{AS} + I_{CS}) - R_{BF}(I_{BS} + I_{BR}) \\ - R_{GF}(I_{AS} + I_{AR} + I_{BS} + I_{BR} + I_{CS} + I_{CR}) = 0 \end{aligned} \quad (7)$$

$$\begin{aligned} V_{CS} - Z_{SS} \cdot I_{CS} - Z_{MS}(I_{AS} + I_{BS}) \\ - m \cdot Z_S \cdot I_{CS} - m \cdot Z_M(I_{AS} + I_{BS}) - R_{CF}(I_{CS} + I_{CR}) \\ - R_{GF}(I_{AS} + I_{AR} + I_{BS} + I_{BR} + I_{CS} + I_{CR}) = 0 \end{aligned}$$

Putting the six linear equations into matrix form yields the six-by-six linear system given in (8) through (12). The solution of this linear system results in six complex numbers representing the currents measured by Relays S and R. These solutions are easily obtained by using modern computer software (via matrix inversion and other linear algebra techniques).

$$\begin{bmatrix} V_{AS} - V_{AR} \\ V_{BS} - V_{BR} \\ V_{CS} - V_{CR} \\ V_{AS} \\ V_{BS} \\ V_{CS} \end{bmatrix} = \begin{bmatrix} [\text{UL}] & [\text{UR}] \\ [\text{BL}] & [\text{BR}] \end{bmatrix} \cdot \begin{bmatrix} I_{AS} \\ I_{BS} \\ I_{CS} \\ I_{AR} \\ I_{BR} \\ I_{CR} \end{bmatrix} \quad (8)$$

$$[\text{UL}] = \begin{bmatrix} Z_{SS} + m \cdot Z_S & Z_{MS} + m \cdot Z_M & Z_{MS} + m \cdot Z_M \\ Z_{MS} + m \cdot Z_M & Z_{SS} + m \cdot Z_S & Z_{MS} + m \cdot Z_M \\ Z_{MS} + m \cdot Z_M & Z_{MS} + m \cdot Z_M & Z_{SS} + m \cdot Z_S \end{bmatrix} \quad (9)$$

$$[\text{UR}] = \begin{bmatrix} -Z_{SR} - (1-m)Z_S & -Z_{MR} - (1-m)Z_M & -Z_{MR} - (1-m)Z_M \\ -Z_{MR} - (1-m)Z_M & -Z_{SR} - (1-m)Z_S & -Z_{MR} - (1-m)Z_M \\ -Z_{MR} - (1-m)Z_M & -Z_{MR} - (1-m)Z_M & -Z_{SR} - (1-m)Z_S \end{bmatrix} \quad (10)$$

$$[\text{BL}] = \begin{bmatrix} Z_{SS} + m \cdot Z_S + R_{AF} + R_{GF} & Z_{MS} + m \cdot Z_M + R_{GF} & Z_{MS} + m \cdot Z_M + R_{GF} \\ Z_{MS} + m \cdot Z_M + R_{GF} & Z_{SS} + m \cdot Z_S + R_{BF} + R_{GF} & Z_{MS} + m \cdot Z_M + R_{GF} \\ Z_{MS} + m \cdot Z_M + R_{GF} & Z_{MS} + m \cdot Z_M + R_{GF} & Z_{SS} + m \cdot Z_S + R_{CF} + R_{GF} \end{bmatrix} \quad (11)$$

$$[\text{BR}] = \begin{bmatrix} R_{AF} + R_{GF} & R_{GF} & R_{GF} \\ R_{GF} & R_{BF} + R_{GF} & R_{GF} \\ R_{GF} & R_{GF} & R_{CF} + R_{GF} \end{bmatrix} \quad (12)$$

Having solved for the currents, we can now determine the phase voltages at the S and R buses by taking the voltage drops over the source impedances, as shown in (13).

$$\begin{aligned} V_{AS_relay} &= V_{AS} - Z_{SS} \cdot I_{AS} - Z_{MS} \cdot (I_{BS} + I_{CS}) \\ V_{BS_relay} &= V_{BS} - Z_{SS} \cdot I_{BS} - Z_{MS} \cdot (I_{AS} + I_{CS}) \\ V_{CS_relay} &= V_{CS} - Z_{SS} \cdot I_{CS} - Z_{MS} \cdot (I_{AS} + I_{BS}) \\ V_{AR_relay} &= V_{AR} - Z_{SR} \cdot I_{AR} - Z_{MR} \cdot (I_{BR} + I_{CR}) \\ V_{BR_relay} &= V_{BR} - Z_{SR} \cdot I_{BR} - Z_{MR} \cdot (I_{AR} + I_{CR}) \\ V_{CR_relay} &= V_{CR} - Z_{SR} \cdot I_{CR} - Z_{MR} \cdot (I_{AR} + I_{BR}) \end{aligned} \quad (13)$$

At this point, the phase-domain solution has yielded complex numbers that represent the six voltages and six currents that correspond to the measurements taken by the virtual relays under steady-state fault conditions. These voltages and currents can be converted into time-varying, ac signals by using secondary test sets and associated software programs. Test software programs typically allow users to specify the secondary test signals in a complex format and are thus easily paired with the solution approach presented in this section. For relay testing, it is often useful to generate signals at the secondary level within the simulator (e.g., using 67 V for the line-to-neutral source voltage magnitude and entering secondary impedance parameters).

Implementing the phase-domain solution requires an up-front investment in the form of writing equations and forming the system matrix. Care must be taken to properly account for the coupling interactions between the three phases of the power system and the transmission line. In exchange, the phase-domain solver allows all ten common shunt faults to be

simulated with a single circuit topology. One general linear system is all that is required for basic distance-element testing. Given that a solver (phase- or sequence-domain) is likely to be implemented on a digital computer today, the single topology offered by the phase-domain solution can be considerably more convenient than the decoupling offered by symmetrical components. Modern computers make it easy to solve relatively large linear systems with complex-valued matrix entries.

So far, we have considered transmission lines with ideal transposition, resulting in identical mutual impedances between the three phases. Consequently, the voltage drops in a particular sequence network depend only on the currents in that sequence network. If the line is not ideally transposed, the mutual impedances are not identical, and the result is a set of coupled sequence networks (with non-zero, off-diagonal terms in the sequence impedance matrix). For example, for an untransposed line, the positive-sequence current can induce a zero-sequence voltage drop. In order to derive exact results in such a case, engineers would be forced to write systems of equations in the sequence domain, which would resemble the coupled phase-domain equations given previously in this section. While it is possible to neglect the coupling between sequence networks and still derive reasonably accurate results for an untransposed line, the fundamental advantage of symmetrical components is somewhat undermined in this case.

In contrast, the phase-domain solution is explicitly built around these coupling interactions. In the case of an untransposed line, we simply modify the impedance matrices and corresponding voltage drop equations so that they take a more general form. Equation (14) shows how the impedance matrices are updated from the ideally transposed line case to the

more general case that accommodates untransposed lines. Conversions for the two system source impedances are similar but with the impedance terms having additional S and R subscripts.

$$\begin{bmatrix} Z_S & Z_M & Z_M \\ Z_M & Z_S & Z_M \\ Z_M & Z_M & Z_S \end{bmatrix} \rightarrow \begin{bmatrix} Z_{AA} & Z_{AB} & Z_{AC} \\ Z_{BA} & Z_{BB} & Z_{BC} \\ Z_{CA} & Z_{CB} & Z_{CC} \end{bmatrix} \quad (14)$$

These substitutions can be made in the linear system derivation, allowing (8) through (12) to be expressed as shown in (15) through (19), respectively.

The more general phase-domain solution can be used to test the behavior of protective relay elements (which generally assume line transposition) for faults on untransposed lines. This solution (with generalized impedance parameters) gives accurate results for such cases. These tests can provide insights into the effects of coupling between sequence networks and can be useful for checking related relay settings.

Thus far, we have focused solely on faults in the forward direction, as seen by the relays on either end of a single transmission line. Starting with the general phase-domain solution obtained previously, it is possible to create additional buses and relays in the power system based on the calculated voltages and currents at the line ends. This effectively allows users to simulate multiple series transmission line sections, each with its own pair of relays. Any fault on such a system

appears forward to some relays and reverse to others. In this way, reverse faults can be simulated without any need to revise the general solution procedure. The following steps provide an example of such a process (refer to Fig. 8):

1. Employ the general phase-domain solution described thus far using twice the actual line impedance in the system solution ($Z' = 2 \cdot Z$, where Z' is entered as the line impedance in the solver). Note that the relays under test are set with Z as the line impedance.
2. In the system solver, enter m' as the per-unit fault location, where ($m' = (1 - m)/2$). The m parameter is the desired per-unit fault location seen by the virtual relays. Recall that the general solution presented previously assumes that the fault location is given relative to Relay S.
3. Use the Relay R current for virtual Relay X, and use the negative of the Relay R current for virtual Relay Y. These relationships result from the CT polarities shown in Fig. 8.
4. Calculate the voltage for virtual Relays X and Y as being equal to the Relay R voltage minus the voltage drop from Bus R to the virtual bus at the location of the virtual relays ($V_R - Z \cdot I_R$).
5. Observe that Relay X sees the fault in the forward direction with a measured impedance of $m \cdot Z$, and Relay Y sees the fault in the reverse direction with a measured impedance of $m \cdot Z$.

$$\begin{bmatrix} V_{AS} - V_{AR} \\ V_{BS} - V_{BR} \\ V_{CS} - V_{CR} \\ V_{AS} \\ V_{BS} \\ V_{CS} \end{bmatrix} = \begin{bmatrix} [\text{UL}] & [\text{UR}] \\ [\text{BL}] & [\text{BR}] \end{bmatrix} \cdot \begin{bmatrix} I_{AS} \\ I_{BS} \\ I_{CS} \\ I_{AR} \\ I_{BR} \\ I_{CR} \end{bmatrix} \quad (15)$$

$$[\text{UL}] = \begin{bmatrix} Z_{AAS} + m \cdot Z_{AA} & Z_{ABS} + m \cdot Z_{AB} & Z_{ACS} + m \cdot Z_{AC} \\ Z_{BAS} + m \cdot Z_{BA} & Z_{BBS} + m \cdot Z_{BB} & Z_{BCS} + m \cdot Z_{BC} \\ Z_{CAS} + m \cdot Z_{CA} & Z_{CBS} + m \cdot Z_{CB} & Z_{CCS} + m \cdot Z_{CC} \end{bmatrix} \quad (16)$$

$$[\text{UR}] = \begin{bmatrix} -Z_{AAR} - (1-m)Z_{AA} & -Z_{ABR} - (1-m)Z_{AB} & -Z_{ACR} - (1-m)Z_{AC} \\ -Z_{BAR} - (1-m)Z_{BA} & -Z_{BBR} - (1-m)Z_{BB} & -Z_{BCR} - (1-m)Z_{BC} \\ -Z_{CAR} - (1-m)Z_{CA} & -Z_{CBR} - (1-m)Z_{CB} & -Z_{CCR} - (1-m)Z_{CC} \end{bmatrix} \quad (17)$$

$$[\text{BL}] = \begin{bmatrix} Z_{AAS} + m \cdot Z_{AA} + R_{AF} + R_{GF} & Z_{ABS} + m \cdot Z_{AB} + R_{GF} & Z_{ACS} + m \cdot Z_{AC} + R_{GF} \\ Z_{BAS} + m \cdot Z_{BA} + R_{GF} & Z_{BBS} + m \cdot Z_{BB} + R_{BF} + R_{GF} & Z_{BCS} + m \cdot Z_{BC} + R_{GF} \\ Z_{CAS} + m \cdot Z_{CA} + R_{GF} & Z_{CBS} + m \cdot Z_{CB} + R_{GF} & Z_{CCS} + m \cdot Z_{CC} + R_{CF} + R_{GF} \end{bmatrix} \quad (18)$$

$$[\text{BR}] = \begin{bmatrix} R_{AF} + R_{GF} & R_{GF} & R_{GF} \\ R_{GF} & R_{BF} + R_{GF} & R_{GF} \\ R_{GF} & R_{GF} & R_{CF} + R_{GF} \end{bmatrix} \quad (19)$$

The preceding description uses shorthand notation to describe the currents, voltages, and impedances on the system. In actuality, the calculations must account for all of the coupling interactions that are present, as in the other derivations presented in this section. The detailed calculations are very similar to those already discussed.

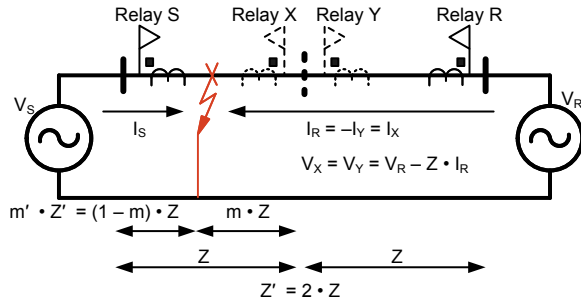


Fig. 8. Creating virtual relays to simulate reverse faults

V. SHUNT FAULT TEST RESULTS

To test the performance of the single-line, phase-domain solver on an actual relay, we generated fault signals for various fault types (both in forward and reverse directions). Fault signals were applied to the local relay (Relay S) using a test set (see Fig. 1).

A symmetrically transposed and homogeneous system with a source impedance ratio of 0.5 was simulated. The line and source setting parameters are specified in Table I. Zone 1 and Zone 2 were set to 80 percent and 120 percent of the line length, respectively. Zone 3 was set farther than the Zone 2 of the remote relay.

As Table II illustrates, the relay operated correctly with accurate directionality and fault location for all the test cases. This serves as a validation of the phase-domain model.

TABLE I
TEST SYSTEM DETAILS

Line and Source Parameters	Source End (S)		Line		Remote End (R)	
	Magnitude (ohms primary)	Angle (degrees)	Magnitude (ohms primary)	Angle (degrees)	Magnitude (ohms primary)	Angle (degrees)
Z_1	18.93	86	37.86	86	18.93	86
Z_0	69.91	76.5	139.82	76.5	69.91	76.5
Z_S	35.81	79.834	71.621	79.834	35.81	79.834
Z_M	17.11	73.011	34.22	73.011	17.11	73.011

TABLE II
SUMMARY OF SHUNT FAULT CASES TESTED ON THE TRANSMISSION LINE

Fault Case	Fault Type	Fault Resistance (ohms primary)	Direction Forward (F)/ Reverse (R)	Location Applied (% of length)	Fault Location Calculated by Relay (% of length)
1	AG	20	F	7	7.05
2	BG	30	F	15	15.02
3	CG	50	F	20	20.03
4	AB	15	F	35	35.01
5	BC	25	F	45	45.01
6	CA	10	F	55	55
7	ABG	5	F	65	65.01
8	BCG	8	F	75	75.02
9	CAG	0	F	90	90
10	ABC	0	F	99.5	99.42
11	AG	25	R	-10	-10.03
12	BC	30	R	-15	-15.03
13	CAG	20	R	-22.5	-22.66
14	ABC	0	R	-29	-28.97

VI. SOLUTION FOR PARALLEL TRANSMISSION LINES

We can expand the solution from Section IV to cover a system with mutually coupled parallel lines. Fig. 9 shows a single-line diagram of such a system. For simplicity, both lines are identical and are ideally transposed, resulting in one self-impedance parameter (Z_S) and one mutual impedance parameter (Z_M). The system source impedances are modeled similarly (as transposed transmission line segments). These impedances reflect the self-interactions and mutual interactions between the three phases of each transmission line. There is also a single, mutual impedance parameter (Z_{MP}) that reflects the coupling between the two lines. The implicit assumption behind the single, line-to-line mutual impedance is that the distance between the two lines is much greater than the distance between the phase conductors on either line. The two lines share common buses (and thus common voltages) on both ends.

The S terminal current is denoted as I_S , the R terminal current is denoted as I_R , and the parallel line current is denoted as I_P . The general phase-domain fault circuit (not shown in full detail) is positioned on the line between Terminals S and R at a per-unit distance m relative to the S terminal. Because there is no shunt capacitance modeled in the system, the current on the unfaulted line (I_P) is uniform over the line. The S source current is the sum of the Relay S current and the parallel line current ($I_S + I_P$). The R source current is the difference between the Relay R current and the parallel line current ($I_R - I_P$).

Depending on the relative flow directions of the zero-sequence currents in the faulted line and the unfaulted line, the distance elements in the relays at Buses S and R can either overreach or underreach. The next section explores this phenomenon in more detail. See [6] for more information on zero-sequence mutual coupling and its effects on transmission line protection.

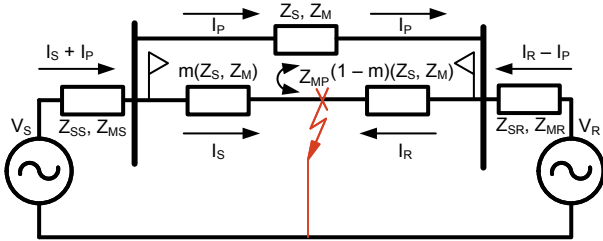


Fig. 9. System with two parallel transmission lines and common buses

In the double-circuit system of Fig. 9, there are nine principal unknowns: I_S (A, B, C), I_R (A, B, C), and I_P (A, B, C). The subsequent unknowns are the voltages at the S and R buses, which are readily calculated once the currents have been solved. We therefore must solve a nine-by-nine system consisting of nine linear equations. For each phase (A, B, C), three equations are written, which are summarized as follows (note that there is some flexibility in writing these equations):

- An equation relating the fault-point voltages as seen from the S and R sides of the system (line voltage drops are calculated on the faulted line).

- A KVL loop starting on the S side and dropping through the fault circuit (line voltage drops are calculated on the faulted line).
- An equation relating the Bus R voltages as seen from the S and R sides of the system (line voltage drops are calculated on the unfaulted line).

These equations are shown for Phase A in the remainder of this section. The equations for Phases B and C are similar. Equation (20) shows the fault voltages as seen from the S and R sides.

$$\begin{aligned} V_{AF_S} = & V_{AS} - Z_{SS}(I_{AS} + I_{AP}) \\ & - Z_{MS}(I_{BS} + I_{BP} + I_{CS} + I_{CP}) \\ & - m \cdot Z_S \cdot I_{AS} - m \cdot Z_M(I_{BS} + I_{CS}) \\ & - m \cdot Z_{MP}(I_{AP} + I_{BP} + I_{CP}) \end{aligned}$$

$$\begin{aligned} V_{AF_R} = & V_{AR} - Z_{SR}(I_{AR} - I_{AP}) \\ & - Z_{MR}(I_{BR} - I_{BP} + I_{CR} - I_{CP}) \\ & - (1-m)Z_S \cdot I_{AR} \\ & - (1-m)Z_M(I_{BR} + I_{CR}) \\ & + (1-m)Z_{MP}(I_{AP} + I_{BP} + I_{CP}) \end{aligned} \quad (20)$$

$$V_{AF_S} = V_{AF_R} \rightarrow V_{AF_S} - V_{AF_R} = 0$$

The KVL loop through the fault circuit is shown in (21).

The results of equating the Bus R voltages, as seen from the S and R sides, are shown in (22).

$$\begin{aligned} & V_{AS} - Z_{SS}(I_{AS} + I_{AP}) - Z_{MS}(I_{BS} + I_{BP} + I_{CS} + I_{CP}) \\ & - m \cdot Z_S \cdot I_{AS} - m \cdot Z_M(I_{BS} + I_{CS}) \\ & - m \cdot Z_{MP}(I_{AP} + I_{BP} + I_{CP}) \\ & - R_{AF}(I_{AS} + I_{AR}) \\ & - R_{GF}(I_{AS} + I_{AR} + I_{BS} + I_{BR} + I_{CS} + I_{CR}) = 0 \end{aligned} \quad (21)$$

$$\begin{aligned} V_{AR_S} = & V_{AS} - Z_{SS}(I_{AS} + I_{AP}) \\ & - Z_{MS}(I_{BS} + I_{BP} + I_{CS} + I_{CP}) \\ & - Z_S \cdot I_{AP} - Z_M(I_{BP} + I_{CP}) \\ & - m \cdot Z_{MP}(I_{AS} + I_{BS} + I_{CS}) \\ & + (1-m)Z_{MP}(I_{AR} + I_{BR} + I_{CR}) \end{aligned} \quad (22)$$

$$\begin{aligned} V_{AR_R} = & V_{AR} - Z_{SR}(I_{AR} - I_{AP}) \\ & - Z_{MR}(I_{BR} - I_{BP} + I_{CR} - I_{CP}) \end{aligned}$$

$$V_{AR_S} = V_{AR_R} \rightarrow V_{AR_S} - V_{AR_R} = 0$$

Representing the nine linear equations in matrix form yields (23) through (32).

$$\begin{bmatrix} V_{AS} - V_{AR} \\ V_{BS} - V_{BR} \\ V_{CS} - V_{CR} \\ V_{AS} \\ V_{BS} \\ V_{CS} \\ V_{AS} - V_{AR} \\ V_{BS} - V_{BR} \\ V_{CS} - V_{CR} \end{bmatrix} = \begin{bmatrix} [\text{UL}] & [\text{UM}] & [\text{UR}] \\ [\text{ML}] & [\text{MM}] & [\text{MR}] \\ [\text{BL}] & [\text{BM}] & [\text{BR}] \end{bmatrix} \begin{bmatrix} I_{AS} \\ I_{BS} \\ I_{CS} \\ I_{AR} \\ I_{BR} \\ I_{CR} \\ I_{AP} \\ I_{BP} \\ I_{CP} \end{bmatrix} \quad (23)$$

$$[\text{UL}] = \begin{bmatrix} Z_{SS} + m \cdot Z_S & Z_{MS} + m \cdot Z_M & Z_{MS} + m \cdot Z_M \\ Z_{MS} + m \cdot Z_M & Z_{SS} + m \cdot Z_S & Z_{MS} + m \cdot Z_M \\ Z_{MS} + m \cdot Z_M & Z_{MS} + m \cdot Z_M & Z_{SS} + m \cdot Z_S \end{bmatrix} \quad (24)$$

$$[\text{UM}] = \begin{bmatrix} -Z_{SR} - (1-m)Z_S & -Z_{MR} - (1-m)Z_M & -Z_{MR} - (1-m)Z_M \\ -Z_{MR} - (1-m)Z_M & -Z_{SR} - (1-m)Z_S & -Z_{MR} - (1-m)Z_M \\ -Z_{MR} - (1-m)Z_M & -Z_{MR} - (1-m)Z_M & -Z_{SR} - (1-m)Z_S \end{bmatrix} \quad (25)$$

$$[\text{UR}] = \begin{bmatrix} Z_{SS} + Z_{SR} + Z_{MP} & Z_{MS} + Z_{MR} + Z_{MP} & Z_{MS} + Z_{MR} + Z_{MP} \\ Z_{MS} + Z_{MR} + Z_{MP} & Z_{SS} + Z_{SR} + Z_{MP} & Z_{MS} + Z_{MR} + Z_{MP} \\ Z_{MS} + Z_{MR} + Z_{MP} & Z_{MS} + Z_{MR} + Z_{MP} & Z_{SS} + Z_{SR} + Z_{MP} \end{bmatrix} \quad (26)$$

$$[\text{ML}] = \begin{bmatrix} Z_{SS} + m \cdot Z_S + R_{AF} + R_{GF} & Z_{MS} + m \cdot Z_M + R_{GF} & Z_{MS} + m \cdot Z_M + R_{GF} \\ Z_{MS} + m \cdot Z_M + R_{GF} & Z_{SS} + m \cdot Z_S + R_{BF} + R_{GF} & Z_{MS} + m \cdot Z_M + R_{GF} \\ Z_{MS} + m \cdot Z_M + R_{GF} & Z_{MS} + m \cdot Z_M + R_{GF} & Z_{SS} + m \cdot Z_S + R_{CF} + R_{GF} \end{bmatrix} \quad (27)$$

$$[\text{MM}] = \begin{bmatrix} R_{AF} + R_{GF} & R_{GF} & R_{GF} \\ R_{GF} & R_{BF} + R_{GF} & R_{GF} \\ R_{GF} & R_{GF} & R_{CF} + R_{GF} \end{bmatrix} \quad (28)$$

$$[\text{MR}] = \begin{bmatrix} Z_{SS} + m \cdot Z_{MP} & Z_{MS} + m \cdot Z_{MP} & Z_{MS} + m \cdot Z_{MP} \\ Z_{MS} + m \cdot Z_{MP} & Z_{SS} + m \cdot Z_{MP} & Z_{MS} + m \cdot Z_{MP} \\ Z_{MS} + m \cdot Z_{MP} & Z_{MS} + m \cdot Z_{MP} & Z_{SS} + m \cdot Z_{MP} \end{bmatrix} \quad (29)$$

$$[\text{BL}] = \begin{bmatrix} Z_{SS} + m \cdot Z_{MP} & Z_{MS} + m \cdot Z_{MP} & Z_{MS} + m \cdot Z_{MP} \\ Z_{MS} + m \cdot Z_{MP} & Z_{SS} + m \cdot Z_{MP} & Z_{MS} + m \cdot Z_{MP} \\ Z_{MS} + m \cdot Z_{MP} & Z_{MS} + m \cdot Z_{MP} & Z_{SS} + m \cdot Z_{MP} \end{bmatrix} \quad (30)$$

$$[\text{BM}] = \begin{bmatrix} -Z_{SR} - (1-m)Z_{MP} & -Z_{MR} - (1-m)Z_{MP} & -Z_{MR} - (1-m)Z_{MP} \\ -Z_{MR} - (1-m)Z_{MP} & -Z_{SR} - (1-m)Z_{MP} & -Z_{MR} - (1-m)Z_{MP} \\ -Z_{MR} - (1-m)Z_{MP} & -Z_{MR} - (1-m)Z_{MP} & -Z_{SR} - (1-m)Z_{MP} \end{bmatrix} \quad (31)$$

$$[\text{BR}] = \begin{bmatrix} Z_{SS} + Z_S + Z_{SR} & Z_{MS} + Z_M + Z_{MR} & Z_{MS} + Z_M + Z_{MR} \\ Z_{MS} + Z_M + Z_{MR} & Z_{SS} + Z_S + Z_{SR} & Z_{MS} + Z_M + Z_{MR} \\ Z_{MS} + Z_M + Z_{MR} & Z_{MS} + Z_M + Z_{MR} & Z_{SS} + Z_S + Z_{SR} \end{bmatrix} \quad (32)$$

Once all nine currents have been solved for, the phase voltages at Buses S and R can be calculated as shown in (33) (these are the relay voltages).

$$\begin{aligned}
 V_{AS_relay} &= V_{AS} - Z_{SS}(I_{AS} + I_{AP}) \\
 &\quad - Z_{MS}(I_{BS} + I_{BP} + I_{CS} + I_{CP}) \\
 V_{BS_relay} &= V_{BS} - Z_{SS}(I_{BS} + I_{BP}) \\
 &\quad - Z_{MS}(I_{AS} + I_{AP} + I_{CS} + I_{CP}) \\
 V_{CS_relay} &= V_{CS} - Z_{SS}(I_{CS} + I_{CP}) \\
 &\quad - Z_{MS}(I_{AS} + I_{AP} + I_{BS} + I_{BP}) \\
 V_{AR_relay} &= V_{AR} - Z_{SR}(I_{AR} - I_{AP}) \\
 &\quad - Z_{MR}(I_{BR} - I_{BP} + I_{CR} - I_{CP}) \\
 V_{BR_relay} &= V_{BR} - Z_{SR}(I_{BR} - I_{BP}) \\
 &\quad - Z_{MR}(I_{AR} - I_{AP} + I_{CR} - I_{CP}) \\
 V_{CR_relay} &= V_{CR} - Z_{SR}(I_{CR} - I_{CP}) \\
 &\quad - Z_{MR}(I_{AR} - I_{AP} + I_{BR} - I_{BP})
 \end{aligned} \tag{33}$$

VII. TEST RESULTS FOR FAULTS ON A DOUBLE-CIRCUIT SYSTEM

For a system with two parallel transmission lines, zero-sequence mutual coupling has an effect on the distance elements and fault location. We can study this effect by considering three scenarios. Consider a homogeneous system with parallel lines and common buses at both ends.

A. Scenario 1

When a line-to-ground fault is applied close to the local end on the system, as shown in Fig. 10, the zero-sequence current in the parallel line is out of phase with the zero-sequence current in the faulted line (measured by Relay S).

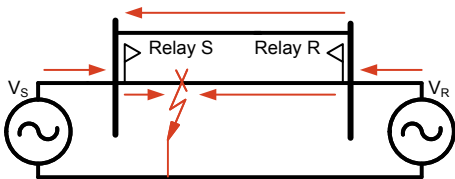


Fig. 10. Mutual coupling Scenario 1

This causes the voltage measured by Relay S to be smaller than what the relay would see in the absence of a parallel line. In turn, this causes the relay to overreach, as is evident from the single-ended fault location equation shown in (34) [7]. Reducing the measured relay voltage reduces the numerator term, which artificially decreases the measured impedance [6]. When a phase-to-phase fault occurs, there is no zero-sequence

current flow in the adjacent line, and correspondingly, there are no reach problems.

$$\begin{aligned}
 \text{Fault Location (pu)} &= \\
 &= \frac{\text{Im}[V_{AS_relay} \cdot I_{2S}^*]}{\text{Im}[(I_{AS} + k_0 \cdot I_{0S}) \cdot Z_{1L} \cdot I_{2S}^*]} \tag{34}
 \end{aligned}$$

B. Scenario 2

When a line-to-ground fault is applied close to the remote end on the system, as shown in Fig. 11, the zero-sequence current in the parallel line is in phase with the zero-sequence current in the faulted line (measured by Relay S).

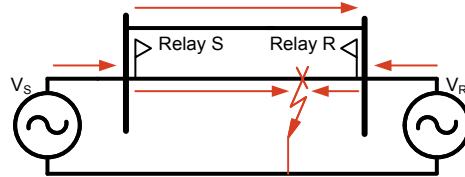


Fig. 11. Mutual coupling Scenario 2

This causes the voltage measured by Relay S to be greater than what the relay would see in the absence of a parallel line. In turn, this causes the relay to underreach. Once more, the relays experience no reach problems for ungrounded phase faults.

C. Scenario 3

When a line-to-ground fault is applied exactly halfway between the local and remote buses, as shown in Fig. 12, the symmetry of the faulted system prohibits the flow of zero-sequence current in the parallel line (recall that the test system is perfectly symmetrical).

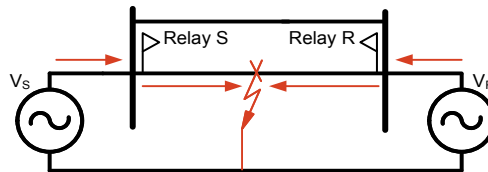


Fig. 12. Mutual coupling Scenario 3

In this scenario, the relays experience no reach problems for grounded or ungrounded faults.

D. Results

We simulated several faults for each of the three scenarios using the double-circuit, phase-domain solver. The results are summarized in Table III. Scenario 1 corresponds to faults at 30 percent of the line length. Scenario 2 corresponds to faults at 90 percent of the line length. Scenario 3 corresponds to faults at 50 percent of the line length.

As evident from Table III, the fault location is essentially perfect for faults at the midpoint of the line. We notice the overreaching and underreaching effects for faults associated with Scenarios 1 and 2, respectively. It is important to note that only the ground faults caused the reach problems in the relay in these two scenarios.

TABLE III
SUMMARY OF SHUNT FAULT CASES TESTED ON THE PARALLEL TRANSMISSION LINE

Fault Case	Fault Type	Fault Resistance (ohms primary)	Direction Forward (F)/ Reverse (R)	Location Applied (percent)	Fault Location Calculated by Relay (percent)
1	AG	10	F	30	29.65
2	BC	10	F	30	30.06
3	AG	10	F	50	50.06
4	BC	10	F	50	50.04
5	AG	10	F	90	96.61
6	BC	10	F	90	89.98

Fig. 13 illustrates the reach behavior for ground faults over the entire line length. Numerous faults were simulated (using the phase-domain solver) along the length of the line from Bus S to Bus R. The Terminal S signals from the simulation were applied to a physical relay and into (34). Fault location results obtained from both are plotted in per unit of the actual fault location.

We can clearly observe the overreaching and underreaching effects for faults below and above 50 percent of the line length, respectively. Greater coupling distance associated with farther fault distance aggravates the reach problems. This explains why the error is larger for faults beyond 50 percent of the line length. These results add credibility to the accuracy of the double-circuit, phase-domain solver.

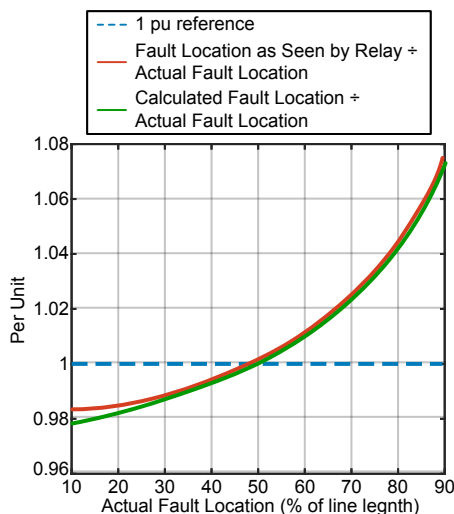


Fig. 13. Effect of zero-sequence current in parallel lines

VIII. DERIVING A TIME-DOMAIN, STATE-SPACE SOLVER

We have now derived several solutions that apply under ac steady-state fault conditions. Such solutions are suited to testing traditional, phasor-based protective relays. In this section, we derive time-domain representations of the steady-state solutions presented previously.

Consider the simple circuit shown in Fig. 14, where an ac source is connected in series with a resistor and an inductor. In ac steady-state conditions, the resistance and the inductive reactance combine in quadrature to form a complex impedance. The voltage drop across the series RL (resistive-inductive) combination is expressed as a single, complex term, equal to the product of the complex current and the complex circuit impedance. The use of capital letters indicates the ac steady-state quantities.

The second circuit of Fig. 14 shows the time-domain equivalent circuit. The voltage and current quantities are correspondingly denoted with lower case letters. Both the voltage and the current are time-varying scalars, and the voltage drop in the circuit consists of two parts: a resistive drop ($R \cdot i$) and an inductive drop ($L \cdot di / dt$).

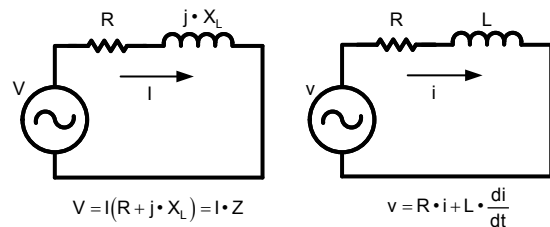


Fig. 14. AC steady-state and time-domain equivalent circuits

We now examine the general transmission line voltage drop equations in a time-domain context starting with steady-state equations. Once more, the ac steady-state voltage drop relationship is shown in (35).

$$\begin{bmatrix} V_A \\ V_B \\ V_C \end{bmatrix} = \begin{bmatrix} Z_{AA} & Z_{AB} & Z_{AC} \\ Z_{BA} & Z_{BB} & Z_{BC} \\ Z_{CA} & Z_{CB} & Z_{CC} \end{bmatrix} \cdot \begin{bmatrix} I_A \\ I_B \\ I_C \end{bmatrix} \quad (35)$$

In each phase of the transmission line, the voltage drop consists of one complex self-impedance term and two complex mutual impedance terms. Expanding the Phase A equation from (35) yields (36).

$$V_A = Z_{AA} \cdot I_A + Z_{AB} \cdot I_B + Z_{AC} \cdot I_C \quad (36)$$

As in Fig. 14, each of the three complex voltage drop terms can be expressed as a sum of the two scalar voltage drop terms in the time domain, yielding (37).

$$\begin{aligned} V_A = & R_{AA} \cdot i_A + L_{AA} \cdot \frac{di_A}{dt} + R_{AB} \cdot i_B \\ & + L_{AB} \cdot \frac{di_B}{dt} + R_{AC} \cdot i_C + L_{AC} \cdot \frac{di_C}{dt} \end{aligned} \quad (37)$$

We now apply similar transformations to the general steady-state solution for a two-source system with a single transmission line. Once more, the system has the general form shown in (38). Note that (38), (39), and (40) have a six-by-six matrix dimension.

$$\begin{bmatrix} V_{AS} - V_{AR} \\ V_{BS} - V_{BR} \\ V_{CS} - V_{CR} \\ V_{AS} \\ V_{BS} \\ V_{CS} \end{bmatrix} = [Z] \cdot \begin{bmatrix} I_{AS} \\ I_{BS} \\ I_{CS} \\ I_{AR} \\ I_{BR} \\ I_{CR} \end{bmatrix} \quad (38)$$

Applying the time-domain transformation results in (39) (note the lower-case convention). The dot convention in this equation is used to denote the time-derivative of an array of currents, and correspondingly, an array of current time-derivatives.

$$\begin{bmatrix} v_{AS} - v_{AR} \\ v_{BS} - v_{BR} \\ v_{CS} - v_{CR} \\ v_{AS} \\ v_{BS} \\ v_{CS} \end{bmatrix} = [R] \cdot \begin{bmatrix} i_{AS} \\ i_{BS} \\ i_{CS} \\ i_{AR} \\ i_{BR} \\ i_{CR} \end{bmatrix} + [L] \cdot \begin{bmatrix} \dot{i}_{AS} \\ \dot{i}_{BS} \\ \dot{i}_{CS} \\ \dot{i}_{AR} \\ \dot{i}_{BR} \\ \dot{i}_{CR} \end{bmatrix} \quad (39)$$

Rearranging the terms in (39) provides (40). In (40), the C matrix is simply a matrix of constants that implements the source voltage subtractions, allowing the source voltage array to be represented in a simpler form.

$$[L] \cdot \begin{bmatrix} \dot{i}_{AS} \\ \dot{i}_{BS} \\ \dot{i}_{CS} \\ \dot{i}_{AR} \\ \dot{i}_{BR} \\ \dot{i}_{CR} \end{bmatrix} = [C] \cdot \begin{bmatrix} v_{AS} \\ v_{BS} \\ v_{CS} \\ v_{AR} \\ v_{BR} \\ v_{CR} \end{bmatrix} - [R] \cdot \begin{bmatrix} i_{AS} \\ i_{BS} \\ i_{CS} \\ i_{AR} \\ i_{BR} \\ i_{CR} \end{bmatrix} \quad (40)$$

Equation (41) is a further condensation of (40). The resistance and inductance terms follow the same subscript conventions used in previous sections.

$$[L] \cdot \dot{[i]} = [C] \cdot [v] - [R] \cdot [i] \quad (41)$$

Matrix descriptions are provided in (42) through (52). Matrix L reflects the line and source parameters and is thus constant throughout the entire simulation (in both prefault and fault states). Matrix R (specifically submatrices R_BL and R_BR) contains the fault resistance parameters, which are updated during the transition from the prefault to fault state.

The matrix equation in (42) is a state-space representation of the power system with the following three key components:

- State variables are the time-domain system currents (i_{AS} , i_{BS} , i_{CS} , i_{AR} , i_{BR} , i_{CR}) and are the primary variables that are solved for.
- Forcing functions are the time-domain system source voltages (v_{AS} , v_{BS} , v_{CS} , v_{AR} , v_{BR} , v_{CR}). They are known because they are explicitly specified within the simulator program.
- Expressions are for the time-derivatives (dot terms) of the state variables in terms of the state variables and the forcing functions.

$$[L] = \begin{bmatrix} [L_UL] & [L_UR] \\ [L_BL] & [L_BR] \end{bmatrix} \quad (42)$$

$$[L_UL] = \begin{bmatrix} L_{AAS} + m \cdot L_{AA} & L_{ABS} + m \cdot L_{AB} & L_{ACS} + m \cdot L_{AC} \\ L_{BAS} + m \cdot L_{BA} & L_{BBS} + m \cdot L_{BB} & L_{BCS} + m \cdot L_{BC} \\ L_{CAS} + m \cdot L_{CA} & L_{CBS} + m \cdot L_{CB} & L_{CCS} + m \cdot L_{CC} \end{bmatrix} \quad (43)$$

$$[L_UR] = \begin{bmatrix} -L_{AAR} - (1-m) \cdot L_{AA} & -L_{ABR} - (1-m) \cdot L_{AB} & -L_{ACR} - (1-m) \cdot L_{AC} \\ -L_{BAR} - (1-m) \cdot L_{BA} & -L_{BBR} - (1-m) \cdot L_{BB} & -L_{BCR} - (1-m) \cdot L_{BC} \\ -L_{CAR} - (1-m) \cdot L_{CA} & -L_{CBR} - (1-m) \cdot L_{CB} & -L_{CCR} - (1-m) \cdot L_{CC} \end{bmatrix} \quad (44)$$

$$[L_BL] = \begin{bmatrix} L_{AAS} + m \cdot L_{AA} & L_{ABS} + m \cdot L_{AB} & L_{ACS} + m \cdot L_{AC} \\ L_{BAS} + m \cdot L_{BA} & L_{BBS} + m \cdot L_{BB} & L_{BCS} + m \cdot L_{BC} \\ L_{CAS} + m \cdot L_{CA} & L_{CBS} + m \cdot L_{CB} & L_{CCS} + m \cdot L_{CC} \end{bmatrix} \quad (45)$$

$$[L_BR] = \begin{bmatrix} 0 & 0 & 0 \\ 0 & 0 & 0 \\ 0 & 0 & 0 \end{bmatrix} \quad (46)$$

$$[\mathbf{R}] = \begin{bmatrix} [\mathbf{R_UL}] & [\mathbf{R_UR}] \\ [\mathbf{R_BL}] & [\mathbf{R_BR}] \end{bmatrix} \quad (47)$$

$$[\mathbf{R_UL}] = \begin{bmatrix} \mathbf{R_{AAS}} + m \cdot \mathbf{R_{AA}} & \mathbf{R_{ABS}} + m \cdot \mathbf{R_{AB}} & \mathbf{R_{ACS}} + m \cdot \mathbf{R_{AC}} \\ \mathbf{R_{BAS}} + m \cdot \mathbf{R_{BA}} & \mathbf{R_{BBS}} + m \cdot \mathbf{R_{BB}} & \mathbf{R_{BCS}} + m \cdot \mathbf{R_{BC}} \\ \mathbf{R_{CAS}} + m \cdot \mathbf{R_{CA}} & \mathbf{R_{CBS}} + m \cdot \mathbf{R_{CB}} & \mathbf{R_{CCS}} + m \cdot \mathbf{R_{CC}} \end{bmatrix} \quad (48)$$

$$[\mathbf{R_UR}] = \begin{bmatrix} -\mathbf{R_{AAR}} - (1-m) \cdot \mathbf{R_{AA}} & -\mathbf{R_{ABR}} - (1-m) \cdot \mathbf{R_{AB}} & -\mathbf{R_{ACR}} - (1-m) \cdot \mathbf{R_{AC}} \\ -\mathbf{R_{BAR}} - (1-m) \cdot \mathbf{R_{BA}} & -\mathbf{R_{BBR}} - (1-m) \cdot \mathbf{R_{BB}} & -\mathbf{R_{BCR}} - (1-m) \cdot \mathbf{R_{BC}} \\ -\mathbf{R_{CAR}} - (1-m) \cdot \mathbf{R_{CA}} & -\mathbf{R_{CBR}} - (1-m) \cdot \mathbf{R_{CB}} & -\mathbf{R_{CCR}} - (1-m) \cdot \mathbf{R_{CC}} \end{bmatrix} \quad (49)$$

$$[\mathbf{R_BL}] = \begin{bmatrix} \mathbf{R_{AAS}} + m \cdot \mathbf{R_{AA}} + \mathbf{R_{AF}} + \mathbf{R_{GF}} & \mathbf{R_{ABS}} + m \cdot \mathbf{R_{AB}} + \mathbf{R_{GF}} & \mathbf{R_{ACS}} + m \cdot \mathbf{R_{AC}} + \mathbf{R_{GF}} \\ \mathbf{R_{BAS}} + m \cdot \mathbf{R_{BA}} + \mathbf{R_{GF}} & \mathbf{R_{BBS}} + m \cdot \mathbf{R_{BB}} + \mathbf{R_{BF}} + \mathbf{R_{GF}} & \mathbf{R_{BCS}} + m \cdot \mathbf{R_{BC}} + \mathbf{R_{GF}} \\ \mathbf{R_{CAS}} + m \cdot \mathbf{R_{CA}} + \mathbf{R_{GF}} & \mathbf{R_{CBS}} + m \cdot \mathbf{R_{CB}} + \mathbf{R_{GF}} & \mathbf{R_{CCS}} + m \cdot \mathbf{R_{CC}} + \mathbf{R_{CF}} + \mathbf{R_{GF}} \end{bmatrix} \quad (50)$$

$$[\mathbf{R_BR}] = \begin{bmatrix} \mathbf{R_{AF}} + \mathbf{R_{GF}} & \mathbf{R_{GF}} & \mathbf{R_{GF}} \\ \mathbf{R_{GF}} & \mathbf{R_{BF}} + \mathbf{R_{GF}} & \mathbf{R_{GF}} \\ \mathbf{R_{GF}} & \mathbf{R_{GF}} & \mathbf{R_{CF}} + \mathbf{R_{GF}} \end{bmatrix} \quad (51)$$

$$\mathbf{C} = \begin{bmatrix} 1 & 0 & 0 & -1 & 0 & 0 \\ 0 & 1 & 0 & 0 & -1 & 0 \\ 0 & 0 & 1 & 0 & 0 & -1 \\ 1 & 0 & 0 & 0 & 0 & 0 \\ 0 & 1 & 0 & 0 & 0 & 0 \\ 0 & 0 & 1 & 0 & 0 & 0 \end{bmatrix} \quad (52)$$

Knowing the present values of the state variables and forcing functions is equivalent to knowing how the state variables are changing. The state variables can be incrementally updated by numerically integrating the time-derivatives. Equations (53) through (56) show an example of this process. The example uses backward Euler integration because this method offers a reasonable balance between simplicity and numerical stability (see [8] for further details). Convergence of the numerical simulation depends only on the convergence of the physical system being simulated. Because there are no significant run-time constraints on the solver program, a sufficiently small simulation time-step compensates for the simplicity of the integration technique. Other integration methods can be used as well, with different methods having distinct simulation time-step size requirements (determined by their inherent stability properties).

In the backward Euler solution, the currents at the present iteration (subscript k) are calculated based on the currents from the previous iteration (subscript $k-1$) and the time-derivatives of the currents from the present iteration (subscript k). The subscript k on the time-derivatives is what distinguishes the backward and forward Euler methods (with the forward

method using $k-1$). In (53), Δt represents the simulation time-step.

$$[\mathbf{i}]_k = [\mathbf{i}]_{k-1} + \dot{[\mathbf{i}]}_k \cdot \Delta t \quad (53)$$

Premultiplying both sides by the inductance matrix yields (54).

$$[\mathbf{L}] \cdot [\mathbf{i}]_k = [\mathbf{L}] \cdot [\mathbf{i}]_{k-1} + [\mathbf{L}] \cdot \dot{[\mathbf{i}]}_k \cdot \Delta t \quad (54)$$

We recognize the last term of this equation (the $\mathbf{L} \cdot \dot{\mathbf{i}}$ term) as the left side of the state-space equation derived previously in (41). The substitution shown in (55) can therefore be made.

$$[\mathbf{L}] \cdot [\mathbf{i}]_k = [\mathbf{L}] \cdot [\mathbf{i}]_{k-1} + \Delta t \cdot \left[[\mathbf{C}] \cdot [\mathbf{v}]_k - [\mathbf{R}] \cdot [\mathbf{i}]_k \right] \quad (55)$$

Thus, we have an implicit expression for the present value of the current array in terms of the previous value of the current array and the present value of the forcing function (the source voltages). The backward Euler method is also known as an implicit method for this reason. Rearranging (55) into a more convenient form provides (56).

$$\left[[\mathbf{L}] + \Delta t \cdot [\mathbf{R}] \right] \cdot [\mathbf{i}]_k = [\mathbf{L}] \cdot [\mathbf{i}]_{k-1} + \Delta t \cdot [\mathbf{C}] \cdot [\mathbf{v}]_k \quad (56)$$

The right side of (56) consists entirely of known quantities (the old value of the current array and the present forcing function value). Thus, the solution of this linear system yields the updated current array. The remaining solution steps are as follows:

1. Insert the present value of the current back into the state-space equation in (41) to solve for the updated current time-derivatives.
2. Use the present value of both the current and the current time-derivative to update the S and R bus voltages (which are also the relay voltages) by taking voltage drops over the source impedances. This is similar to the approach described previously in this paper, except that now it takes a time-domain form.

Thus, we have transformed the ac steady-state solution for the two-source, single-line system into a direct, time-domain equivalent. For such simple systems, the state-space solution is intuitive and relatively easy to understand. The correspondence between ac steady-state circuit behavior and time-domain circuit behavior is also readily apparent using this method. This solution correctly models the RL circuit behavior under both steady-state and transient conditions.

IX. APPLICATION OF THE PHASE-DOMAIN SOLVER TO THE TESTING OF TIME-DOMAIN, INCREMENTAL QUANTITY-BASED PROTECTION FUNCTION

Time-domain, incremental quantity-based relaying is available and offers notable advantages, such as faster fault clearing [9]. The concept was first employed in the early 1980s in ultra-high-speed directional relays [9] [10] [11]. As explained in [10], [11], [12], [13], and [14], the concept of an incremental quantity is to measure the increment (difference) between the present instantaneous value of a measured quantity and the value from some time in the past. The time difference is in multiples of power system cycles. Reference [13] describes an example incremental quantity, which is shown in (57).

$$\Delta s(t) = s(t) - s(t - p \cdot T) \quad (57)$$

where:

$\Delta s(t)$ is the instantaneous incremental quantity.

$s(t)$ is the measured instantaneous value.

t is the instantaneous time value.

T is the period of the measured quantity.

p is an arbitrary number of power cycles.

Incremental quantities can be used for ultra-high-speed directional relaying and for faulted phase selection. Fault directionality is established by comparing the incremental voltage to the incremental replica current. Reference [13] describes the principle of the incremental quantity-based

directional element. If there is a fault in front of the relay (forward direction), the incremental voltage and incremental current in the faulted phase have opposite polarity. For a fault behind the relay (reverse direction), the incremental voltage and incremental replica current in the faulted phase have the same polarity. These signatures establish the fault directionality.

What happens when we use a test set to apply two sequential sets of steady-state signals (one for the prefault state and one for the fault state) to a time-domain relay without properly considering the state transition? Will the relay element performance match expectations? We can use the steady-state, phase-domain solver (derived in previous sections) to test this. Consider a two-source system connected with a single transmission line shown in Fig. 1 using the same impedance values as shown in Table I. Self-impedance and mutual impedance parameters are derived from the positive- and zero-sequence parameters and are used in the phase-domain solver.

The following two example cases illustrate the behavior of incremental quantity-based directional elements when sequential steady-states are applied to simulate prefault and fault conditions.

A. Case 1

An AG fault is simulated in the forward direction at 30 percent of the line length, as seen by Relay S. The prefault state is 1 second long (note the disturbance in the voltages and currents at the fault inception in Fig. 15) Fig. 16 shows the incremental voltage and current waveforms (with the relevant transition highlighted in blue) measured by Relay S, as well as the forward and reverse directional element assertions.

During the first few milliseconds of the fault, the directional element provides reverse declaration. This behavior is attributed to the artificial discontinuity between the prefault and fault states generated by the secondary test set. Therefore, combining two ac steady-state solutions in a state sequence can yield unexpected results.

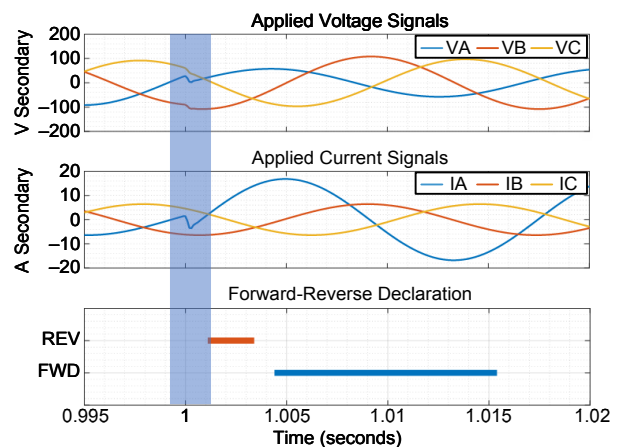


Fig. 15. Voltage and current signals with prefault time of 1 second

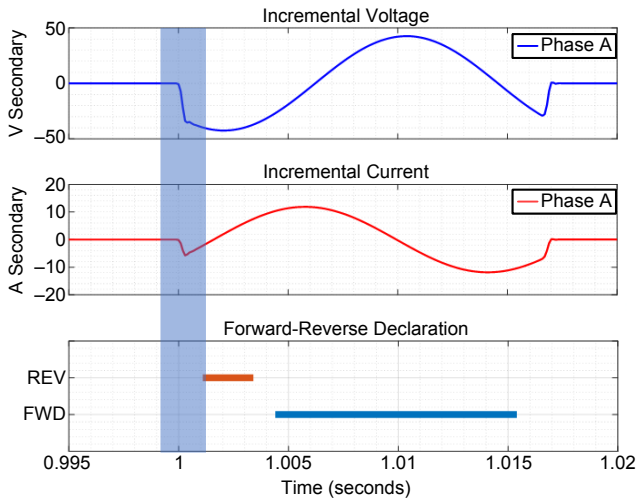


Fig. 16. Incremental voltage and currents with pre-fault time of 1 second (zoomed in)

B. Case 2

Applying the same ac steady-state signals as in Case 1 while changing the pre-fault duration to 1.00136 seconds eliminated the artificial discontinuity at the fault inception, as shown in Fig. 17. Consequently, the fault is declared forward, as expected, with respect to Relay S, and the time-domain protection operates correctly. The incremental voltages and currents are shown in Fig. 18.

Evidently, the pre-fault duration affects the point on the wave at fault inception, which profoundly influences the relationship between the voltage and current incremental quantities when sequential ac steady-states are applied. Similar results are observed for line-to-line faults. Fig. 19 and Fig. 20 show the incremental quantities for bolted CA faults with pre-fault lengths of 1 second and 1.00226 seconds, respectively.

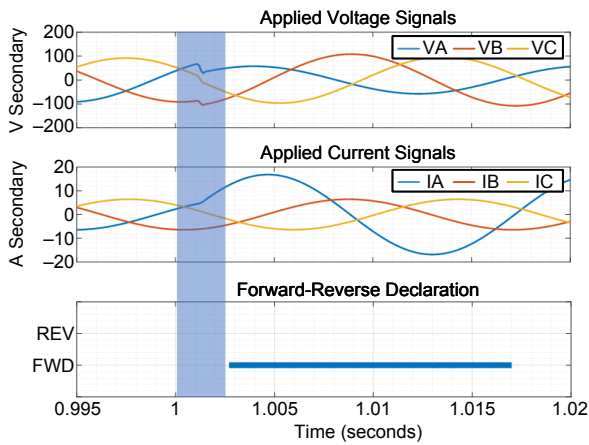


Fig. 17. Voltage and current signals with pre-fault time of 1.00136 seconds

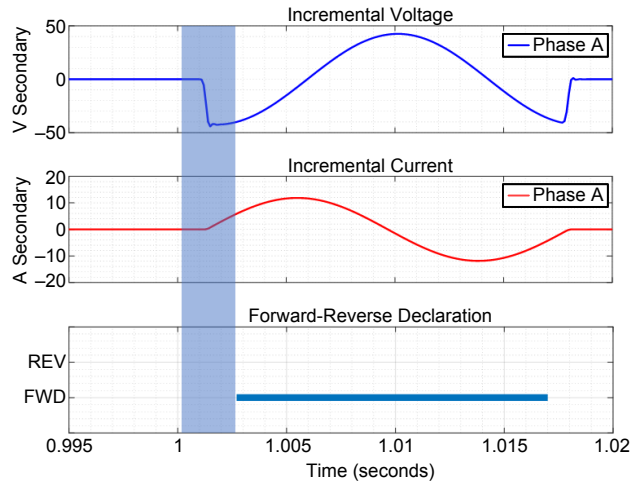


Fig. 18. Incremental voltage and currents with pre-fault time of 1.00136 seconds (zoomed in)

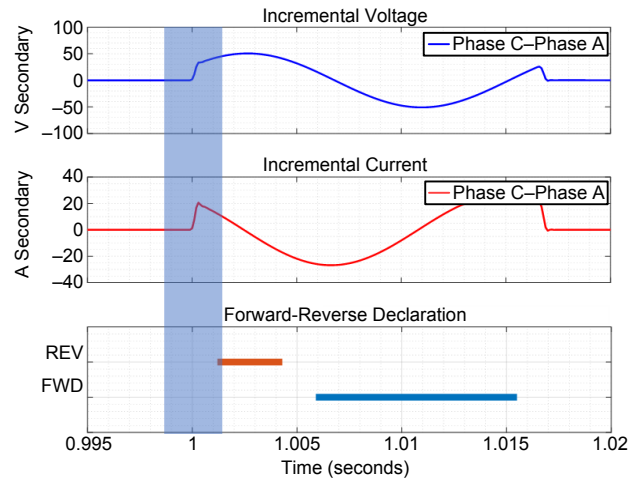


Fig. 19. Line-to-line fault with pre-fault time of 1 second (declared as reverse fault)

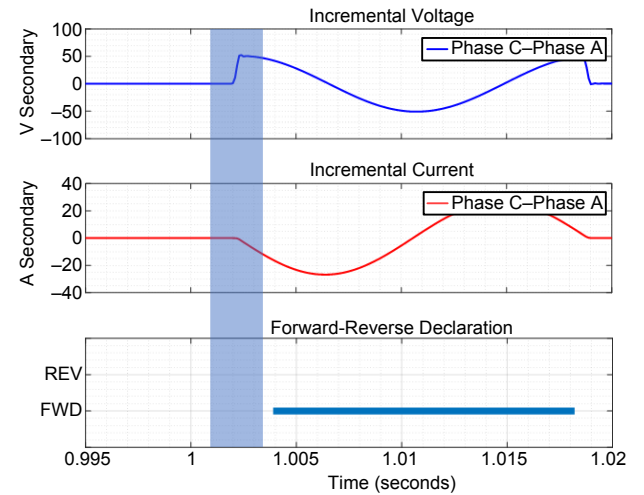


Fig. 20. Line-to-line fault with pre-fault time of 1.00226 seconds (declared as forward fault)

Once again, the same ac steady-state solutions for the prefault and fault signals yield different directional declarations, with the difference being attributable to the prefault length and the resulting point on the wave.

Combining two ac steady-states to simulate the transition from prefault to fault can result in an artificial (nonphysical) discontinuity. This can cause time-domain, incremental quantity-based elements to exhibit unexpected behavior. Possible remedies for this include the following:

- Precisely calculate the prefault length to minimize or eliminate the artificial discontinuity when applying sequential steady-states.
- Use a proper time-domain simulation to generate relay test signals.

The prefault durations for Case 2 (1.00136 seconds for the successful AG trial and 1.00226 seconds for the successful CA trial) were calculated using a methodology described in [15]. Essentially, the prefault duration is calculated to eliminate the problematic discontinuities between ac steady-states. Equation (58) is used to calculate the prefault duration. Observe in Fig. 18 and Fig. 20 that the incremental current changes smoothly, with no abrupt discontinuities, when the prefault time is calculated using this formula. This is true despite the fact that no decaying dc signal is applied.

$$t_0 = \frac{1}{\text{NFREQ}} \cdot \left(\text{NC} - \frac{\text{ang}(\Delta I)}{360^\circ} \right) \quad (58)$$

where:

t_0 is the prefault duration in seconds.

ΔI is the phasor difference between the fault current and the prefault current.

NC is the number of power cycles for the length of prefault at nominal frequency.

NFREQ is the system nominal frequency.

C. Options for Generating Reliable Test Signals

This approach of carefully stitching together two ac steady-states can work well for the commissioning and bench testing of incremental quantity-based protection functions. It is particularly well-suited for testing single-line-to-ground faults because for a single faulted phase, there is only one point on the wave to optimize.

Another method is to use a genuine time-domain solver to generate realistic test signals. Many widely used transient simulation software programs are suitable for this task. As an alternative, this paper presents a state-space solution that accurately models the RL dynamics of a transmission line, requiring minimal settings and modeling complexity.

Instead of outputting complex numbers that correspond to ac steady-states, a time-domain solver generates a stream of scalar data samples that correspond to the waveform data. These data can be packaged into a file format that facilitates secondary-level playback using a test set. The IEEE COMTRADE file format, among others, is suitable for this purpose. The use of a time-domain solver ensures that incremental quantity-based protection functions operate properly, regardless of the fault point on the wave (this is subject to relay design and sensitivity

constraints). This is because the numerical simulation generates the proper decaying dc signal that, in real RL systems, prevents the current from changing abruptly. These solvers also allow both single-phase and multiphase fault loops to be tested with equal ease.

X. USING THE TIME-DOMAIN SOLVER TO TEST TIME-DOMAIN PROTECTION FUNCTIONS

In the previous section, the cases with a prefault length of 1 second proved to be problematic when ac steady-state signals were used to test time-domain, incremental quantity-based protection functions. These cases were recreated using the time-domain solution presented in Section VIII. A simulation time-step of $12.5 \mu\text{s}$ (corresponding to 80 kHz processing) was used, and COMTRADE data were generated at 8 kHz. The following figures show the test result for an AG fault with a prefault time of 1 second (Case 1 from Section IX). The waveforms generated with the time-domain solution (shown in Fig. 21) provide the correct transition from prefault to fault (meaning that the transition reflects the actual transient response of the system). Because the artificial discontinuity is no longer present, the directional element correctly indicates a forward fault (see Fig. 22).

Similar results can be seen for a bolted CA fault with a prefault length of 1 second (see Fig. 23 and Fig. 24). Again, the incremental current transitions smoothly, and the incremental quantities correctly yield a forward declaration.

Table IV shows the incremental quantity-based protection function results for several BCG faults in both the forward and reverse directions. Faults were simulated at 50 percent of the line length, as seen by Relay S. The faults were simulated with various points on the wave at the fault inception in order to illustrate correct directional pickup, regardless of inception angle. The use of a time-domain simulation ensures the correct directional pickup by properly modeling the RL dynamics. We also recreated the results of Table II with the time-domain solver, and they were nearly identical.

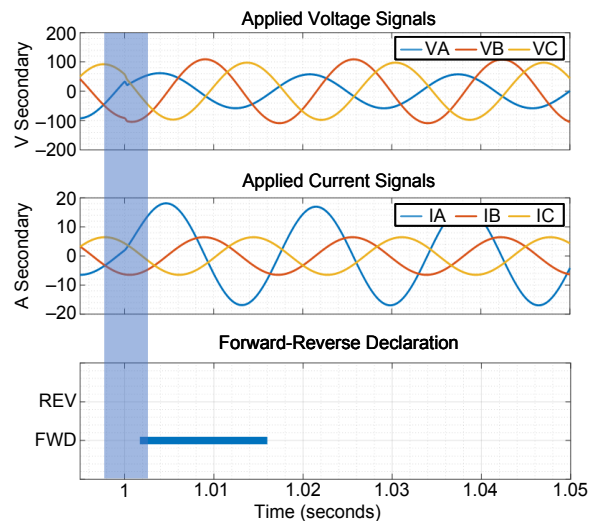


Fig. 21. Time-domain voltage and current signals with prefault time of 1 second for AG fault at 30 percent of line length and with time-domain solver

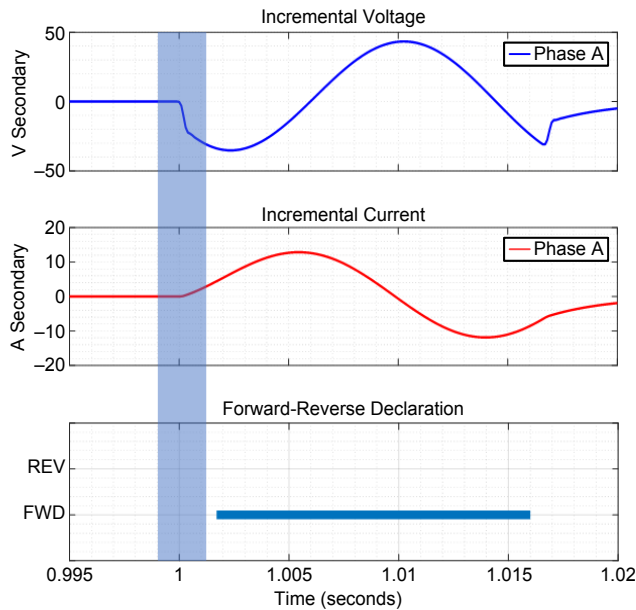


Fig. 22. Incremental voltage and current with prefault time of 1 second for AG fault at 30 percent of line length and with time-domain solver

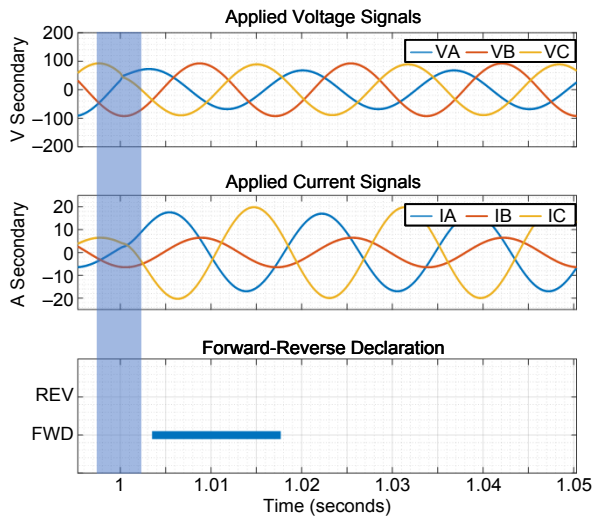


Fig. 23. Time-domain voltage and current signals with a prefault time of 1 second for CA fault at 40 percent of the line length and with time-domain solver

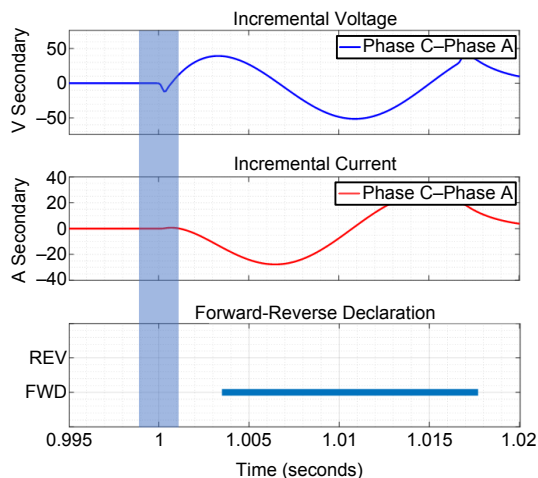


Fig. 24. Incremental voltage and current with prefault time of 1 second for CA fault 40 percent of line length and with time-domain solver

TABLE IV
BC-TO-GROUND FAULT ON VARIOUS POINTS
ON THE WAVE WITH TIME-DOMAIN SOLVER

Number	Point on Wave (degrees)	Simulated Fault Direction	Fault Direction Declared by Relay
1	36	F	F
2	45	F	F
3	90	F	F
4	159	F	F
5	175	F	F
6	192	F	F
7	230	F	F
8	285	F	F
9	333	F	F
10	351	F	F
11	45	R	R
12	90	R	R
13	285	R	R

XI. CONCLUSIONS

Phase-domain analysis of faulted transmission lines requires detailed consideration of the mutual coupling interactions between the three phases (A, B, C). In practice, this entails solving linear systems of a modest size (six-by-six for a two-ended system) with complex-valued matrix coefficients. This was prohibitively difficult before the advent of digital computers, necessitating the use of symmetrical components. Solving three decoupled systems (positive, negative, zero) is considerably easier to do by hand, resulting in the widespread use of symmetrical components in teaching and in practice. Today, symmetrical component techniques remain dominant in university curricula.

Whereas symmetrical components offer decoupling, phase-domain methods allow multiple fault types to be modeled with a single general circuit topology. This can be very convenient in practice, and it contrasts with the multiple topologies required with symmetrical components. In addition, phase-domain analysis minimizes the amount of abstraction required to make models, and the associated equations correspond more directly to basic physics. Because phase-domain analysis explicitly models the phase-to-phase electromagnetic coupling interactions, it is well-suited to model untransposed lines and to generate results for such lines with uncompromised accuracy.

AC steady-state signals derived from phase-domain solvers are ideally suited for performing secondary-level testing on traditional, phasor-based relays. These solvers are advantageous in the following ways:

- One solver handles multiple fault types.

- Modeling complexity is kept to a minimum. Only a few basic parameters are needed (such as the fault location and the self-impedances and mutual impedances of the line and sources).
- Results are displayed in a complex format and can be directly entered into testing software programs.

For time-domain protection function testing, the equations of the steady-state, phase-domain solver can be directly translated into a time-domain, state-space equivalent. This way, the number of modeling parameters remains at a minimum. In conjunction with numerical integration techniques, this solution yields transient waveform data that accurately reflect the prefault to fault transition. Accurate modeling of this transition ensures reliable testing results and does not require fine-tuning of the prefault length and resulting point on the wave.

XII. REFERENCES

- [1] C. L. Fortescue, "Method of Symmetrical Co-Ordinates Applied to the Solution of Polyphase Networks," *Transactions of the American Institute of Electrical Engineers*, Vol. XXXVII, Issue 2, June 1918, pp. 1,027–1,140.
- [2] J. L. Blackburn and T. J. Domin, *Protective Relaying: Principles and Applications*, 3rd ed. CRC Press: Taylor & Francis Group, Boca Raton, FL, 2006.
- [3] E. O. Schweitzer, III, and S. E. Zocholl, "Introduction to Symmetrical Components," proceedings of the 30th Annual Western Protective Relay Conference, Spokane, WA, October 2003.
- [4] P. M. Anderson, *Analysis of Faulted Power Systems*, 1st ed. Iowa State University Press, 1973.
- [5] S. E. Zocholl, "Three-Phase Circuit Analysis and the Mysterious k_0 Factor," proceedings of the 48th Annual Conference for Protective Relay Engineers, College Station, TX, April 1995.
- [6] D. A. Tziouvaras, H. J. Altuve, and F. Calero, "Protecting Mutually Coupled Transmission Lines: Challenges and Solutions," proceedings of the 68th Annual Conference for Protective Relay Engineers, College Station, TX, March 2014.
- [7] O. Avendano, B. Kasztenny, H.J. Altuve, B. Le, and N. Fischer, "Tutorial on Fault Locating Embedded in Line Current Differential Relays – Methods, Implementation, and Application Considerations," proceedings of the 17th Annual Georgia Tech Fault and Disturbance Analysis Conference, Atlanta, GA, April 2014.
- [8] J. C. Butcher, *Numerical Methods for Ordinary Differential Equations*, 2nd ed. John Wiley & Sons, Ltd, Chichester, England, 2008.
- [9] O. E. Lanz, M. Hanggli, G. Bacchini, and F. Engler, "Transient Signals and Their Processing in an Ultra High-Speed Directional Relay for EHV/UHV Transmission Line Protection," *IEEE Transactions on Power Apparatus and Systems*, Vol. PAS-104, Issue 6, June 1985, pp. 1,463–1,473.
- [10] P. G. McLaren, E. Dirks, R. P. Jayasinghe, I. Fernando, G. W. Swift, and Z. Zhang, "A Positive Sequence Directional Element for Numerical Distance Relays," proceedings of the 6th International Conference on Developments in Power System Protection, Nottingham, England, March 1997.
- [11] G. Benmouyal and J. Mahseredjian, "A Combined Directional and Faulted Phase Selector Element Based on Incremental Quantities," *IEEE Transactions on Power Delivery*, Vol. 16, Issue 4, October 2001, pp. 478–484.
- [12] G. Benmouyal and S. Chano, "Characterization of Phase and Amplitude Comparators in UHS Directional Relays," *IEEE Transactions on Power Systems*, Vol. 12, Issue 2, May 1997, pp. 646–653.

- [13] E. O. Schweitzer, III, B. Kasztenny, A. Guzmán, V. Skendzic, and M. V. Mynam, "Speed of Line Protection – Can We Break Free of Phasor Limitations?," proceedings of the 68th Annual Conference for Protective Relay Engineers, College Station, TX, March 2015.
- [14] H. Li and P. G. McLaren, "A Phase Selection Algorithm for an Adaptive Impedance Relay," proceedings of the IEEE Canadian Conference on Electrical and Computer Engineering, Edmonton, Canada, May 1999.
- [15] SEL-T400L Instruction Manual. Available: <https://selinc.com>.

XIII. BIOGRAPHIES

Steven Chase received his bachelor of science degree in electrical engineering from Arizona State University in 2008 and his master of science in electrical engineering degree in 2009. He worked for two years as a substation design intern at Salt River Project, an Arizona water and power utility. He joined Schweitzer Engineering Laboratories, Inc. in 2010, where he works as a lead power engineer in the research and development division. He is a registered professional engineer in the state of Washington.

Sumit Sawai received a bachelor's degree in electrical engineering from the Sardar Patel College of Engineering in Mumbai, India, in 2011 and a master's degree in electrical engineering from Michigan Technological University in Houghton, MI, in 2015. He joined Schweitzer Engineering Laboratories, Inc. in 2015 and holds the position of power engineer in the research and development division. He was an intern at Siemens India Limited in 2014.

Amol Kathe received a bachelor's degree in electrical engineering from Mumbai University in Mumbai, India, in 2006 and earned his master's degree in electrical engineering from Michigan Technological University in Houghton, MI, in 2014. He worked for over five years as a manager at Reliance Infrastructure Limited in the operations department of the energy division. He joined Schweitzer Engineering Laboratories, Inc. in 2014 and holds the position of power engineer in the research and development division.